

<https://helda.helsinki.fi>

---

## Phased laser diode array permits selective excitation of ultrasonic guided waves in coated bone-mimicking tubes

Moilanen, Petro

2017-10-14

---

Moilanen , P , Salmi , A , Kilappa , V , Zhao , Z , Timonen , J & Haeggström , E 2017 , '  
Phased laser diode array permits selective excitation of ultrasonic guided waves in coated  
bone-mimicking tubes ' , Journal of Applied Physics , vol. 122 , no. 14 , 144901 . <https://doi.org/10.1063/1.5007224>

---

<http://hdl.handle.net/10138/308105>

<https://doi.org/10.1063/1.5007224>

---

cc\_by\_nc\_sa

publishedVersion

---

*Downloaded from Helda, University of Helsinki institutional repository.*

*This is an electronic reprint of the original article.*

*This reprint may differ from the original in pagination and typographic detail.*

*Please cite the original version.*

# Phased laser diode array permits selective excitation of ultrasonic guided waves in coated bone-mimicking tubes

Cite as: J. Appl. Phys. **122**, 144901 (2017); <https://doi.org/10.1063/1.5007224>

Submitted: 04 May 2017 . Accepted: 30 September 2017 . Published Online: 10 October 2017

Petro Moilanen, Ari Salmi, Vantte Kilappa, Zuomin Zhao , Jussi Timonen, and Edward Hæggström



View Online



Export Citation



CrossMark

## ARTICLES YOU MAY BE INTERESTED IN

[Phase-delayed laser diode array allows ultrasonic guided wave mode selection and tuning](#)

Journal of Applied Physics **113**, 144904 (2013); <https://doi.org/10.1063/1.4801394>

[Multichannel Multiple Signal Classification for dispersion curves extraction of ultrasonic guided waves](#)

The Journal of the Acoustical Society of America **143**, EL87 (2018); <https://doi.org/10.1121/1.5022699>

[Triboelectric effect: A new perspective on electron transfer process](#)

Journal of Applied Physics **122**, 144302 (2017); <https://doi.org/10.1063/1.5006634>

## Lock-in Amplifiers up to 600 MHz



Zurich  
Instruments



# Phased laser diode array permits selective excitation of ultrasonic guided waves in coated bone-mimicking tubes

Petro Moilanen,<sup>1,2</sup> Ari Salmi,<sup>1</sup> Vantte Kilappa,<sup>2</sup> Zuomin Zhao,<sup>3</sup> Jussi Timonen,<sup>2</sup> and Edward Hægström<sup>1</sup>

<sup>1</sup>Department of Physics, University of Helsinki, P.O. Box 64, Helsinki 00014, Finland

<sup>2</sup>Department of Physics, University of Jyväskylä, P.O. Box 35, Jyväskylä 40014, Finland

<sup>3</sup>Department of Electrical Engineering, University of Oulu, P.O. Box 4500, Oulu 90014, Finland

(Received 4 May 2017; accepted 30 September 2017; published online 10 October 2017)

This paper validates simulation predictions, which state that specific modes could be enhanced in quantitative ultrasonic bone testing. Tunable selection of ultrasonic guided wave excitation is useful in non-destructive testing since it permits the mediation of energy into diagnostically useful modes while reducing the energy mediated into disturbing contributions. For instance, it is often challenging to distinguish and extract the useful modes from ultrasound signals measured in bone covered by a soft tissue. We show that a laser diode array can selectively excite ultrasound in bone mimicking phantoms. A fiber-coupled diode array (4 elements) illuminated two solid tubes (2–3 mm wall thickness) embraced by an opaque soft-tissue mimicking elastomer coating (5 mm thick). A predetermined time delay matching the selected mode and frequency was employed between the outputs of the elements. The generated ultrasound was detected by a 215 kHz piezo receiver. Our results suggest that this array reduces the disturbances caused by the elastomer cover and so pave way to permit non-contacting *in vivo* guided wave ultrasound assessment of human bones. The implementation is small, inexpensive, and robust in comparison with the conventional pulsed lasers. Published by AIP Publishing. <https://doi.org/10.1063/1.5007224>

## I. INTRODUCTION

Guided waves (GWs) have been used for mechanical characterization of biological and man-made structures (Rocha-Gaso *et al.*, 2009; Raghavan and Cesnik, 2007; and Chillara and Lissenden, 2015). Their wave properties, such as long propagation distance and low attenuation together with affordability of the transducers, make GWs a valuable tool for industrial non-destructive evaluation (NDE) and materials science. GW inspection can be done without contacting the sample, for example, with lasers (Davies *et al.*, 1993), which allows the measurement of fragile and hostile (e.g., hot, radioactive) samples.

A problem with GWs is mode selection: With traditional excitation methods, several guided wave modes propagate that overlap (Rose, 2000). Multiple modes bring benefits—different modes have different particle movement, and thus probing different parts and properties of the sample (Alleyne and Cawley, 1992). However, slow modes often overlap with fast modes which arrive earlier, and some modes are naturally easy to excite. This creates a situation where certain modes hide other modes, modes that could contain important information. To solve this problem of choosing a particular mode, we previously proposed a phased laser diode array solution and demonstrated that we could select between the two fundamental Lamb modes ( $A_0$  and  $S_0$ ) propagating on plates (Karppinen *et al.*, 2013). Related techniques of spatial and temporal modulation for mode selection have been investigated in several publications (Grünsteidl *et al.*, 2013; Sharples *et al.*, 2006; Veres *et al.*, 2013; and Song *et al.*, 2016).

Building on our previous research, we next investigated coated structures, both man-made (coated tubes, coated

plates) and natural ones (bone embraced by soft tissue). As an example, bone wall thickness characterization is difficult because of the large number of propagating modes (Moilanen *et al.*, 2008), and thus, it would be beneficial to transfer power from interfering modes to the fundamental flexural guided wave (FFGW; which can be used to estimate wall thickness). Ability to select the excited mode would also be beneficial, for example, coated tubes used in petrochemical, power, and pipeline industries (Yu *et al.*, 2013).

To address these needs, we set out to demonstrate that an array of four pulsed laser diodes can selectively excite guided waves (e.g., FFGW) into a bone-mimicking tube embraced by an opaque soft-tissue mimicking coating. This work strives to introduce an inexpensive laser acoustic GW excitation method that permits fast and flexible mode tuning. Tunability is important for adaptive and reproducible *in vivo* assessment of human subjects.

## II. MATERIALS AND METHODS

### A. Samples

Our two axisymmetric bone phantoms [Fig. 1(b)] (Moilanen *et al.*, 2014) mimic the dimensions of the human radius (Moilanen *et al.*, 2007). The phantoms are 120 mm long and feature 16 mm external diameter and a wall thickness of 2 and 3 mm. The phantoms were custom made of a composite of aluminum oxide powder ( $Al_2O_3$ , 70% mass, 6  $\mu$ m grain size) and epoxy resin (Stycast 1266, Emerson & Cuming). The solid phantoms were coated by a 5 mm thick soft-tissue mimicking layer, made of a 1:1 mixture of silicone elastomer (Sylgard<sup>®</sup> 184; Dow Corning Corp.) and

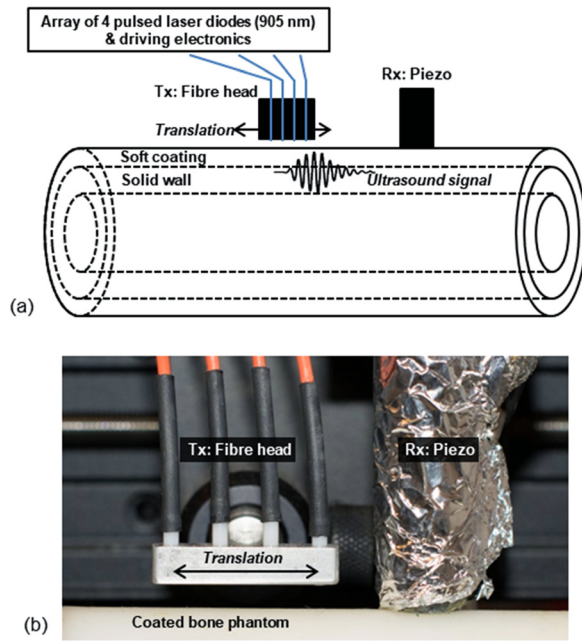


FIG. 1. Experimental setup. The laser beams diverge from the ends of the optical fibers of the array. Each fiber generates a 2 mm wide illuminated spot on the soft coating.

glycerol. Table I lists the elastic (compression velocity  $c_L$ , shear velocity  $c_T$ , and density  $\rho$ ) and optical (absorption coefficient  $\mu_a$ , reduced scattering coefficient  $\mu_s$ , and penetration depth  $1/e_p$ ) properties of the soft and solid materials.

## B. Experimental setup

Figure 1 shows the experimental setup. Light from four pulsed laser diodes (Osram opto semiconductors SPL PL 90\_3 905 nm) was mediated by optical fibers (200  $\mu\text{m}$  diameter, M27L02; Thorlabs) into a fiber head array, featuring 3.5 mm inter-fiber distance. The illuminated spot on the coating was 2 mm in diameter. The laser diodes were successively excited using a tunable time delay, that is, phase delay ( $t_{pd}$ ) (Karppinen *et al.*, 2013). The fiber head (distance to the coating 2 mm) was translated along the long axis of the sample, in 0.5 mm steps, to provide sixty source-receiver distances within 20–50 mm range. The distance was determined from the closest fiber to the center of the receiver. A custom-made piezo transducer (10 mm diameter, 215 kHz center frequency, and 60 kHz bandwidth at  $-6$  dB) was used as receiver. The receiver resided in the far field of the photo-

acoustic source since the near field length for our  $\varnothing = 2$  mm source is  $\ll 1$  mm.

## C. Signal processing

The received spatio-temporal signals were processed in MATLAB (Ver. 7.11, Natick, MA, USA) with 2D-FFT (Alleyn and Cawley, 1991 and Moilanen *et al.*, 2006) to produce mode maps as functions of the wave number and frequency. Spectral maxima in these mode maps, represented by brighter intensities compared with the dark background, represent observed ultrasound modes.

The modulus of the 2D-FFT represented the magnitude of the received ultrasound modes. The magnitude squared provided a power-related quantity and was represented in decibels relative to the average FFGW magnitude. To compare the magnitudes of the experimentally observed ultrasound modes, we analyzed the mode map within five distinct frequency bands. Zone 1 was determined within  $\pm 5\%$  neighborhood (wavenumber direction) along the theoretically predicted dispersion curve of the  $F_{LC}(1,1)$  mode. The spectral maximum of Zone 1 appeared within the 20–40 kHz frequency range. This (experimentally observed) mode has been named “fundamental flexural guided wave” (FFGW) (Moilanen *et al.*, 2013, 2014; and Kilappa *et al.*, 2015). Zone 2 was determined within the  $\pm 5\%$  neighborhood of the  $L_{LC}(0,1)$  mode, and the spectral maximum of Zone 2 appeared within the 35–55 kHz frequency range. This mode, mainly, causes interference that makes it harder to detect the FFGW through the soft coating. Due to the overlapping frequencies, it is not possible to sufficiently reduce this disturbance by (low-pass or band-pass) filtering. Zones 3–5 were determined by another method. The frequency limits were determined by three frequency bands (55–80 kHz, 85–110 kHz, and 170–230 kHz, respectively) and the wavenumber limits from zero to maximum (determined at the center frequency of each band divided by a 4000 m/s slope). These regions of interest (Zones 3–5) were empirically chosen by observing the recorded mode maps so as to consistently group similar patterns of the most energetic spectral maxima and associate these patterns consistently with certain theoretically predicted modes. For details, see Sec. III.

Selective excitation of a chosen mode requires maximizing the power ratio between the mode and other interfering modes that appear at or near the same frequency band. We call this power ratio signal-to-interference ratio (SIR). We optimized SIR by altering the time delay between the excitation of each fiber. The SIR gain was evaluated relative to excitation at  $t_{pd} = 0$ .

## D. Theoretical predictions

Theoretical predictions for modes propagating in a solid tube embraced by a soft coating were determined by a model of traction-free elastic tubes (Gazis, 1959) covered by a finite layer of ideal liquid (Moilanen *et al.*, 2008). We considered the family of longitudinal modes  $L_{LC}(0,i)$  and the family of first order flexural modes  $F_{LC}(1,i)$ , where the subscript LC refers to a liquid coated tube and index  $i = 1, 2, 3$ , etc. The material properties used for the theoretical predictions were consistent with the properties of the bone phantoms.

TABLE I. Elastic and optical properties of the soft and solid materials (Moilanen *et al.*, 2014).

Property	Soft coating	Solid substrate
Compression velocity, $c_L$ (m/s)	$1250 \pm 20$	$2980 \pm 30$
Shear velocity, $c_T$ (m/s)	n/a	$1550 \pm 40$
Mass density, $\rho$ (g/cm <sup>3</sup> )	$1.12 \pm 0.02$	$2.30 \pm 0.01$
Optical absorption coefficient, $\mu_a$ (cm <sup>-1</sup> )	$0.15 \pm 0.05$	$0.30 \pm 0.05$
Reduced scattering coefficient, $\mu_s$ (cm <sup>-1</sup> )	$18 \pm 2$	$6.5 \pm 0.5$
Penetration depth, $1/e_p$ (mm)	$3.3 \pm 0.2$	$1.25 \pm 0.05$



The value of the phase-delay parameter of the phased excitation was predicted as in (Karppinen *et al.*, 2013)

$$t_{pd}(f) = \frac{L_p}{c_{ph}(f)} - n \frac{1}{f}, \quad (1)$$

where  $L_p = 3.5$  mm is the inter-element separation (pitch) of the source array,  $c_{ph}(f)$  is the phase velocity of a chosen mode at frequency  $f$ , and  $n$  is an arbitrary integer ( $n=0$  for the fundamental phase of excitation). Curves determined by Eq. (1) are shown in Fig. 2. Thick lines represent results with  $n=0$  and thin lines results with  $n<0$ . Results with  $n>0$  do not fit within the figure. Phased excitation tuned according to Eq. (1) is expected to maximize the magnitude of a chosen mode relative to the interfering modes. We strive to show that this is the case in experiments with coated tubes.

### III. RESULTS

Figure 3 shows 2D-FFT mode maps at four values of the phase delay parameter, measured on a 3 mm tube. The positions of the bright intensity maxima change with tuning the phase delay parameter. This shows that tuning the phased

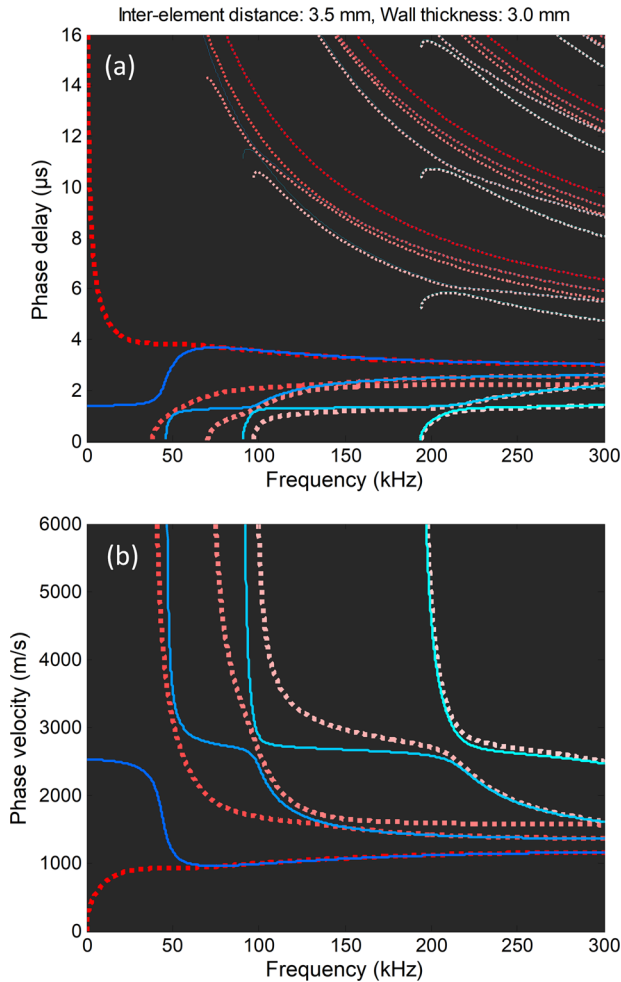


FIG. 2. Theoretically predicted (a) phase delay and (b) phase velocity as a function of frequency in a 3 mm tube with 5 mm coating. Thick lines represent results with  $n=0$  and thin lines results with  $n<0$ . Blue color tones (solid lines) represent longitudinal modes  $L_{LC}(0,i)$  and red color tones (dashed lines) fundamental flexural modes  $F_{LC}(1,i)$ . The values of index  $i = 1, 2, 3, 4$  are indicated by descending levels of color saturation.

excitation affects the coupling of energy into different modes.

Importantly, the positions of the intensity maxima (their peak values) were qualitatively consistent with the theoretically predicted dispersion curves. The results of the analysis of the 2D-FFT mode maps within five distinct zones are presented next.

Figure 4 shows the peak 2D-FFT magnitude within these five zones as a function of the phase delay parameter in 1.9 and 3.0 mm tubes. The color coded lines represent the theoretically predicted modes, as shown in Figs. 2 and 3. Zone 1, associated with a fundamental flexural mode  $F_{LC}(1,1)$ , was depicted by red color. Blue color represents the mixed contributions of L and F modes, the partial roles/contributions of which cannot be distinguished by the present signal processing.

Figure 4(a) shows that the magnitude in Zones 2–5 is maximized when  $t_{pd}$  is 0–2  $\mu$ s. This is qualitatively consistent with the theoretically predicted values of the fundamental phase of excitation ( $n=0$ ), as shown by thick lines in Fig. 2. The fundamental flexural mode in Zone 1 is maximized when  $t_{pd}$  is 4–5  $\mu$ s, which is consistent with predicted  $F_{LC}(1,1)$  curve at  $n=0$  (red thick dashed line) in Fig. 2.

Zone 3 features a second maximum at  $t_{pd} = 13$ –14  $\mu$ s ( $f = 55$ –80 kHz) [Fig. 4(a)], predicted by  $n=-1$  excitation of the  $L_{LC}(0,2)$  mode (Fig. 2). Consistently, the second maximum in Zone 4 at  $t_{pd} = 12$ –13  $\mu$ s ( $f = 85$ –110 kHz) is explained by  $n=-1$  excitation of the  $L_{LC}(0,3)$  mode. Furthermore, the second maximum in Zone 5 at  $t_{pd} = 6$   $\mu$ s ( $f = 170$ –230 kHz) is explained by  $n=-1$  excitation of the  $L_{LC}(0,4)$  mode. The third maximum observed within Zone 5 ( $t_{pd} = 11$ –12  $\mu$ s;  $f = 170$ –230 kHz) is explained by  $n=-2$  excitation of the  $L_{LC}(0,4)$  mode.

As seen in Fig. 4(b), the results were qualitatively similar for another sample featuring a 1.9 mm wall thickness.

Figure 5 shows SIR gain between Zone 1 (FFGW) and Zone 2 modes as a function of phase delay in 3.0 mm and 1.9 mm tubes. The highest SIR gain was  $14.9 \text{ dB} \pm 2.3 \text{ dB}$  (at  $t_{pd} = 6.8$   $\mu$ s) in the 3.0 mm tube and  $15.8 \text{ dB} \pm 1.3 \text{ dB}$  (at  $t_{pd} = 7.1$   $\mu$ s) in the 1.9 mm tube.

### IV. DISCUSSION

We showed that phased photo-acoustic excitation permits tunable and selective mode excitation in coated tube samples, in a manner similar to that we used previously with free plate samples (Karppinen *et al.*, 2013). In coated tubes we observed, within the frequency range of interest, several modes separated into five zones, whereas in the plate, there were only two modes. The observed peak magnitude as a function of time delay parameter value, in each of the five zones, followed the theoretical predictions. These results are important for all applications of guided waves, since different wave modes probe different properties and volumes of the material in question, and thus, it is beneficial to be able to select the probing mode. One example of this is quantitative ultrasonic guided wave assessment of human bones, where a solid tubular waveguide is analyzed through an embracing layer of soft coating, which tends to hamper the

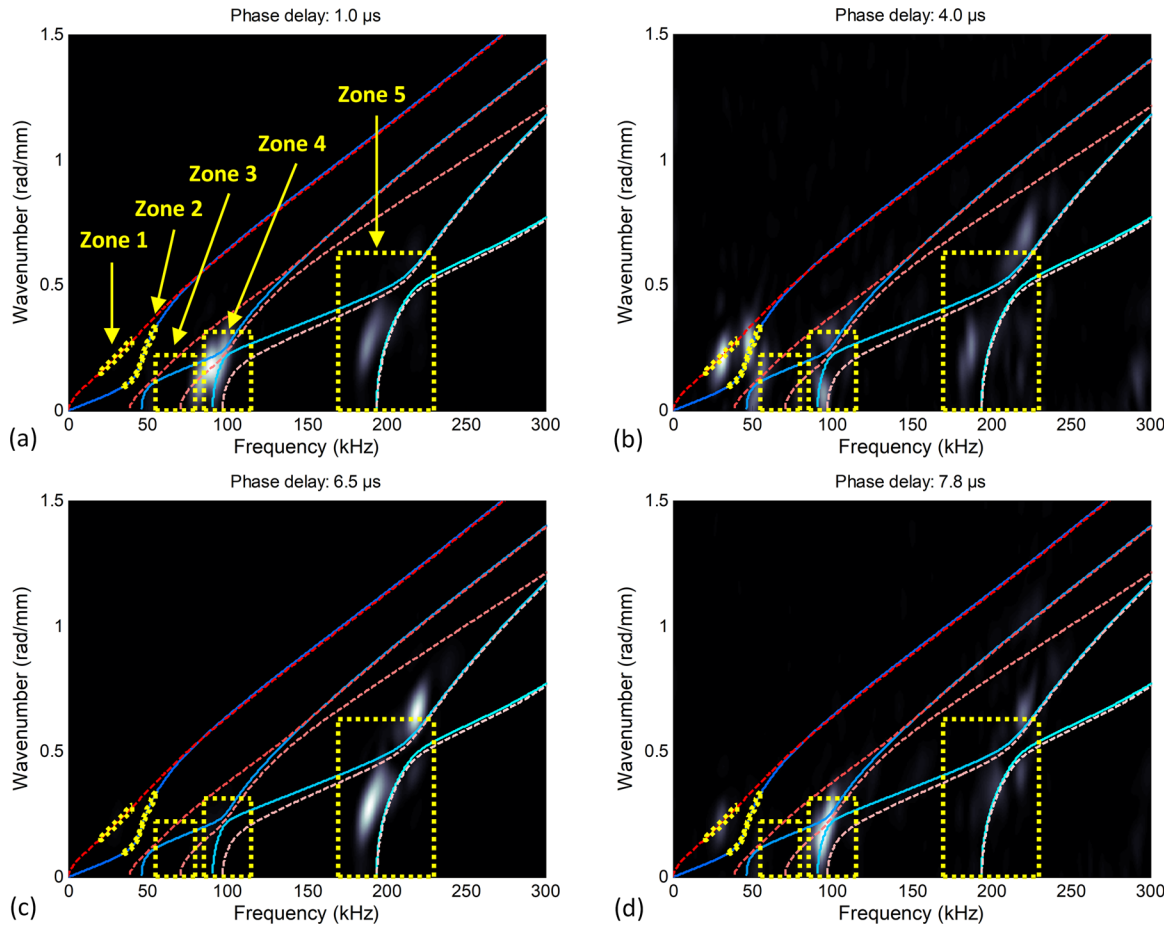


FIG. 3. 2D-FFT mode maps at four values of the phase delay parameter. Results are shown for a 3 mm tube with 5 mm coating. Zones 1 to 5 (regions of interest) are indicated by yellow. Colored curves represent theoretical predictions. Blue color tones (solid lines) represent longitudinal modes  $L_{LC}(0,i)$  and red color tones (dashed lines) fundamental flexural modes  $F_{LC}(1,i)$ . The values of index  $i = 1, 2, 3, 4$  are indicated by descending levels of color saturation.

detection. In our experiments on phantoms, phased excitation permitted 15 dB magnification of the SIR of a clinically relevant FFGW mode. The SIR gain should permit ultrasonic assessment through a thicker layer of soft tissue covering than has been possible thus far.

To evaluate the suitability of the proposed techniques for bone in particular, we tuned the properties (elastic and

optical) of the phantoms to mimic those of cortical bone and soft tissue covering. This resulted in heterogeneous mixtures, which feature the dispersive propagation of bulk waves, whereas the theoretical predictions represent results for non-dispersive media. This fact may explain some of the discrepancy seen between the predicted and experimental results.

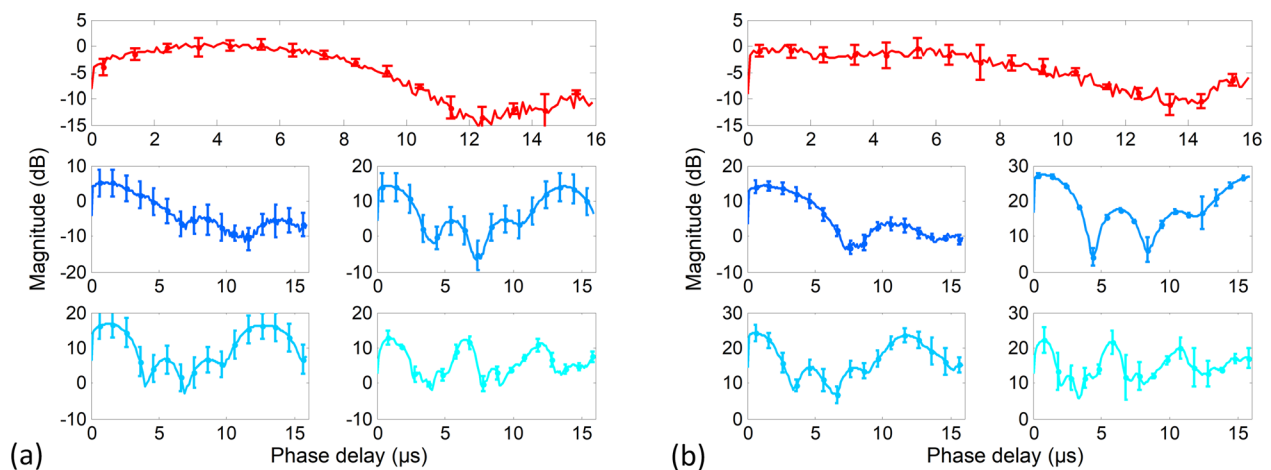


FIG. 4. Magnitudes of five peaks observed in 2D-FFT mode maps as a function of phase delay parameter are shown (a) for a 3.0 mm tube and (b) a 1.9 mm tube. The colors in the five subpanels are consistent with those of the closest theoretically predicted branches that may explain the observed spectral maxima.

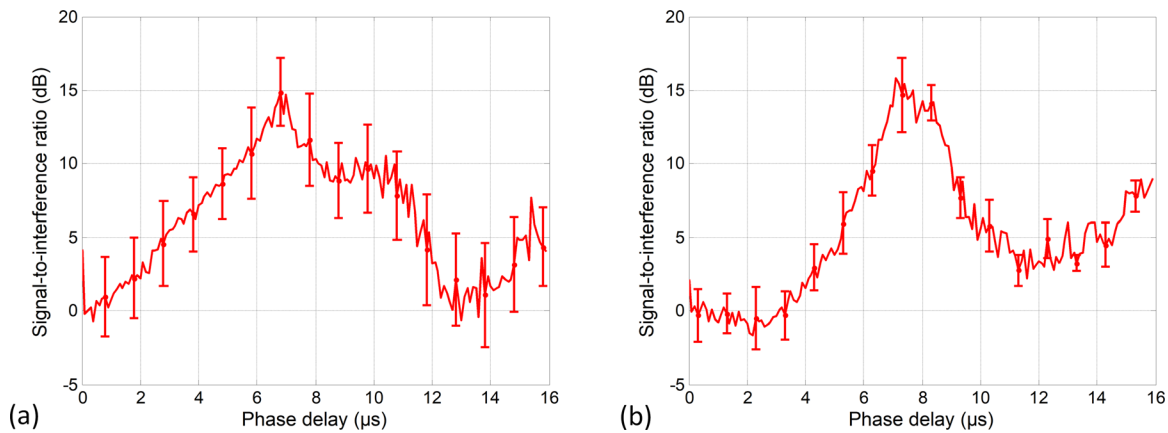


FIG. 5. SIR gain between the peak observed at 20–40 kHz (FFGW) and that observed at 35–55 kHz (closest disturbance). The gain is normalized to SIR at zero phase delay.

Another limitation of the study was that 2D-FFT combined with a short 30 mm range of source-receiver distances results in poor separation of observed modes. The intensity maxima were blurred in the wavenumber domain. We were unable to distinguish which modes were excited and observed. We associated most of the observed modes (zones) to the L family of modes, even though it is evident that F modes may have contributed to our observations as well. An exception was the FFGW in Zone 1, which was clearly related to the  $F_{LC}(1,1)$  mode, consistently with our earlier observations (Moilanen *et al.*, 2014).

We applied 2D-FFT without preprocessing the signal by group-velocity filtering. Therefore, anything that was observed within the time window of reception contributed to the 2D-FFT mode maps.

The results are consistent with recent 2D simulation results in fluid-covered plates (Kilappa *et al.*, 2015). The simulations predicted higher SIR gain (21 dB) than that recorded in our experiments (15 dB). Many factors may explain this difference. The (2D-FFT) signal processing has limited the ability to accurately distinguish modes, and different preprocessing of the signal data was used in the simulating paper. The efficiency of the phased excitation combined with 2D-FFT may be less effective in 3D (experiments) than 2D (simulations) as in 3D there are more modes involved. Nevertheless, the obtained and predicted SIR gains are sufficiently close to show that phased excitation is useful also in real experiments in coated waveguides.

## V. CONCLUSIONS

We introduced an inexpensive laser acoustic GW excitation method that permits fast and flexible mode tuning in coated bone-mimicking tubes. This approach permits rapid adaptive tuning which is an important feature when developing means for reproducible *in vivo* assessment of human subjects. The SIR gain should permit ultrasonic assessment through a thicker layer of soft tissue covering than has been possible thus far. Moreover, the implementation is compact and inexpensive. The presented technique should be useful also with other applications of ultrasonic guided wave non-destructive testing than bone assessment.

## ACKNOWLEDGMENTS

This study was financed by European Regional Funds and the Academy of Finland (Project Nos. 135211, 134897, 135069, and 133183).

- Alleyne, D. and Cawley, P., "A two-dimensional Fourier transform method for the measurement of propagating multimode signals," *J. Acoust. Soc. Am.* **89**(3), 1159–1168 (1991).
- Alleyne, D. N. and Cawley, P., "The interaction of Lamb waves with defects," *IEEE Trans. Ultrason., Ferroelectr. Freq. Control* **39**(3), 381–397 (1992).
- Chillara, V. K. and Lissenden, C. J., "Review of nonlinear ultrasonic guided wave nondestructive evaluation: Theory, numerics, and experiments," *Opt. Eng.* **55**(1), 011002 (2015).
- Davies, S. J., Edwards, C., Taylor, G. S., and Palmer, S. B., "Laser generated ultrasound: Its properties, mechanisms and multifarious applications," *J. Phys. D: Appl. Phys.* **26**, 329–348 (1993).
- Gazis, D. C., "Three dimensional investigation of the propagation of waves in hollow circular cylinders I. Analytical foundation," *J. Acoust. Soc. Am.* **31**(5), 568–573 (1959).
- Grünsteidl, C., Veres, I. A., Roither, J., Burgholzer, P., Murray, T. W., and Berer, T., "Spatial and temporal frequency domain laser-ultrasound applied in the direct measurement of dispersion relations of surface acoustic waves," *Appl. Phys. Lett.* **102**(1), 011103 (2013).
- Karppinen, P., Salmi, A., Moilanen, P., Zhao, Z., Myllylä, R., Timonen, J., and Hægström, E., "Phase-delayed laser diode array allows ultrasonic guided wave mode selection and tuning," *J. Appl. Phys.* **113**, 144904 (2013).
- Kilappa, V., Moilanen, P., Salmi, A., Zhao, Z., Hægström, E., Timonen, J., and Myllylä, R., "Tailoring the excitation of fundamental flexural guided waves in coated bone by phase-delayed array: Two-dimensional simulations," *J. Acoust. Soc. Am.* **137**(3), 1134–1143 (2015).
- Moilanen, P., Kilappa, V., Timonen, J., Salmi, A., Karppinen, P., Hægström, E., Zhao, Z., and Myllylä, R., "Photo-acoustic phase-delayed excitation of guided waves in coated bone phantoms," in *Proceedings of the IEEE International Ultrasonics Symposium* (2013), pp. 2080–2083.
- Moilanen, P., Nicholson, P. H. F., Kilappa, V., Cheng S., and Timonen, J., "Measuring guided waves in long bones: Modeling and experiments in free and immersed plates," *Ultrasound Med. Biol.* **32**, 709–719 (2006).
- Moilanen, P., Nicholson, P. H., Kilappa, V., Cheng, S., and Timonen, J., "Assessment of the cortical bone thickness using ultrasonic guided waves: Modelling and in vitro study," *Ultrasound Med. Biol.* **33**, 254–262 (2007).
- Moilanen, P., Talmant, M., Kilappa, V., Nicholson, P. H. F., Cheng, S., Timonen, J., and Laugier, P., "Modeling the impact of soft tissue on axial transmission measurements of ultrasonic guided waves in long bones," *J. Acoust. Soc. Am.* **124**(4), 2364–2373 (2008).
- Moilanen, P., Zhao, Z., Karppinen, P., Karppinen, T., Kilappa, V., Pirhonen, J., Myllylä, R., Hægström, E., and Timonen, J., "Photo-acoustic excitation and optical detection of fundamental flexural guided wave in coated bone phantoms," *Ultrasound Med. Biol.* **40**(3), 521–531 (2014).

- Raghavan, A. and Cesnik, C. E. S., "Review of guided-wave structural health monitoring," *Shock Vib. Dig.* **39**, 91 (2007).
- Rocha-Gaso, M., March-Iborra, C., Montoya-Baides, A., and Arnau-Vives, A., "Surface generated acoustic wave biosensors for the detection of pathogens: A review," *Sensors* **9**(7), 5740–5769 (2009).
- Rose, J. L., "Guided wave nuances for ultrasonic nondestructive evaluation," *IEEE Trans. Ultrason., Ferroelectr. Freq. Control* **47**(3), 575–583 (2000).
- Sharples, S. D., Clark, M., and Somekh, M. G., "Spatially resolved acoustic spectroscopy for fast noncontact imaging of material microstructure," *Opt. Express* **14**, 10435 (2006).
- Song, X., Moilanen, M., Zhao, Z., Ta, D., Pirhonen, J., Salmi, A., Hæggström, E., Myllylä, R., Timonen, J., and Wang, W., "Coded excitation speeds up the detection of the fundamental flexural guided wave in coated tubes," *AIP Adv.* **6**, 095001 (2016).
- Veres, I. A., Cleary, A., Thursby, G., McKee, C., Armstrong, I., Pierce, G., and Culshaw, B., "Golay code modulation in low-power laser-ultrasound," *Ultrasonics* **53**(1), 122–129 (2013).
- Yu, B., Yang, S., Gan, C., and Lei, H., "A new procedure for exploring the dispersion characteristics of longitudinal guided waves in a multi-layered tube with weak interface," *J. Nondestruct. Eval.* **32**, 263–276 (2013).